A hardware and software system for MRI applications requiring external device data

Karyna Isaieva, Marc Fauvel, Nicolas Weber, Pierre-andré Vuissoz, Jacques Felblinger, Julien Oster, Freddy Odille

FULL PAPER

Accepted in Magnetic Resonance in Medicine, pre-print version (2022)

A hardware and software system for MRI applications requiring external device data

Karyna Isaieva[1,†], Marc Fauvel[2,†], Nicolas Weber[1], Pierre-André Vuissoz[1], Jacques Felblinger[1,2], Julien Oster[1] and Freddy Odille[1,2]

Purpose: Numerous MRI applications require data from external devices. Such devices are often independent of the MRI system, so synchronizing these data with the MRI data is often tedious and limited to offline use. In this work, a hardware and software system is proposed for acquiring data from external devices during MR imaging, for use online (in real-time) or offline.

Methods: The hardware includes a set of external devices - electrocardiography (ECG) devices, respiration sensors, microphone, electronics of the MR system etc. - using various channels for data transmission (analog, digital, optical fibers), all connected to a server through a USB hub. The software is based on a flexible client-server architecture, allowing real-time processing pipelines to be configured and executed. Communication protocols and data formats are proposed, in particular for transferring the external device data to an open-source reconstruction software (Gadgetron), for online image reconstruction using external physiological data. The system performance is evaluated in terms of accuracy of the recorded signals and delays involved in the real-time processing tasks. Its flexibility is shown with various applications.

Results: The real-time system had low delays and jitters (on the order of 1 ms). Example MRI applications using external devices included: prospectively-gated cardiac cine imaging, multi-modal acquisition of the vocal tract (image, sound and respiration) and online image reconstruction with nonrigid motion correction.

Conclusion: The performance of the system and its versatile architecture make it suitable for a wide range of MRI applications requiring online or offline use of external device data.

Keywords: Physiological data, Hardware, Software, Real-time, Signal processing.

INTRODUCTION

A number of MRI applications require data from accessory devices to be acquired simultaneously with the imaging data. For example, physiological data are required for patient motion management in cardiac or abdominal imaging, and can be provided by electrocardiography (ECG) devices or respiratory motion sensors, such as pneumatic belts. Other accessory devices, that operate independently of the MR scanner, have been developed for obtaining complementary information about patient motion, such as optical tracking systems (1), inertial measurement units (including accelerometers, gyroscopes and possibly magnetometers) (2), or ultrasound devices (3). Optical microphones are also used during real-time imaging of speech in order to match dynamic images of the vocal tract to sound recordings (4–6). For MR safety applications, specific measurements are often required such as temperature, radiofrequency (RF) field, electric field, or magnetic field.

While modern MRI systems dispose a set of accessory devices, they are usually limited to a narrow bandwidth ECG, a respiratory belt and a finger pulse device. Their construction implies standard installation which might be impossible in some cases (e.g. pregnant women in lateral position, utilization of a tight flexible coil), and allows monitoring of only respiratory and heart activities. Moreover, being designed for clinical use, they offer no control over data acquisition and post-processing, which can be critical for some applications. For example, standard ECG processing can lead to incorrect QRS detection in case of steep gradient waveforms; no control over respiratory belt signal gain and offset (to avoid signal saturation) is available. Thus, often, accessory devices are third-party systems, which offer more flexibility, however have no communication interface with the MR system, or limited ones. Dedicated computer and electronics systems, as well as communication interfaces, are needed for use in either real-time/online applications or retrospective/offline applications. In the following we review several exemplary applications with the aim to derive typical requirements for such systems.

Example applications that require real-time processing and communication include ECG denoising (7–10) and detection of the QRS complex (11–13), in order to trigger the MR sequence to the heart rate prospectively. The trigger is provided to the MR system by a TTL signal. The delays introduced by the real-time processing system, as defined by the latency (mean delay) and jitter (standard deviation of the delay), should be significantly lower that the temporal resolution of cardiac MR imaging, which is typically above 20 ms. Real-time display of the denoised ECG is also desired during anesthesia, cardiac stress MRI, or interventional MRI. Prospective motion correction (14) using external devices also relies on a real-time setup to modulate the MRI pulses (RF and magnetic field gradient pulses) in order to compensate for the effect of patient motion during spatial encoding. Low latency is also desired, ideally to be equal to the repetition time (TR) of the sequence or lower, i.e. 3 to 5 ms, though in practice it is limited by the time needed to process video images, e.g. 60 to 150 ms in (15). Software communication interfaces need to be defined with the vendor-dependent pulse sequence program in order to provide certain motion parameters (e.g. translations, rotations).

[†]These authors contributed equally to this work

[1]IADI, INSERM and Université de Lorraine, Nancy, France;
[2]CIC-IT 1433, INSERM, Université de Lorraine and CHRU Nancy, Nancy, France;

This work was supported by the Investments for the Future program (ANR-15-RHU-0004), projects BraCoil (ANR-17-CE19-0022) and Full3DTalkingHead (ANR-20-CE23-0008), and the ERACVD Joint Translational Call 2019, MEIDIC-VTACH (ANR-19-ECVD-0004) of ANR (Agence Nationale de la Recherche), France. The authors thank INSERM, CPER IT2MP, Région Lorraine and FEDER. We also thank Coralie Bringtown for her help with ECG acquisition and analysis.

*Correspondence to: Freddy Odille, IADI, Inserm U947 CIC-IT 1433, Bâtiment Recherche, CHRU de Nancy Brabois, Rue du Morvan, 54511, Vandoeuvre-lès-Nancy, France. E-mail: freddy.odille@inserm.fr.

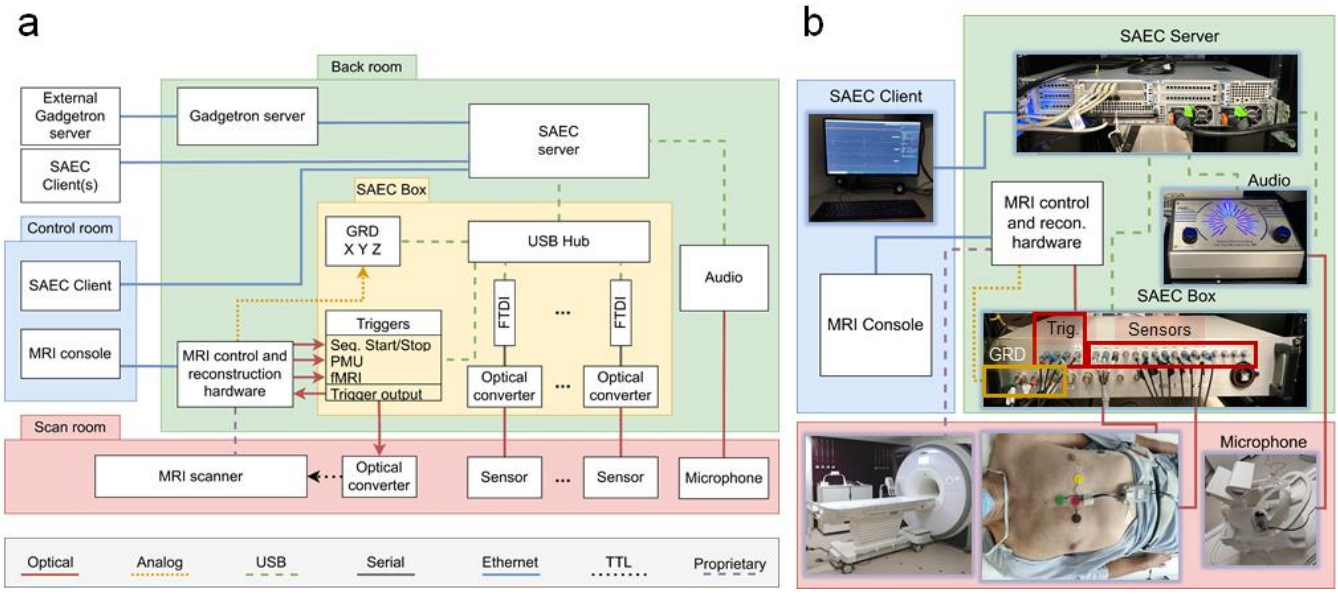

Figure 1. a) Scheme of the hardware components which compose, and which interact with the SAEC system. b) Simplified hardware scheme with photo-illustrations.

Example applications that require offline synchronization of the MR and accessory device data include motion-corrected reconstruction techniques (16,17), in which the patient motion state (as determined by the amplitude or phase of a motion signal) need to be known for each acquired k-space sample; real-time speech imaging, in which sound recordings need to be aligned with the dynamic imaging scene, possibly using sequence start and stop information; analysis of functional MRI (fMRI) data simultaneously acquired with electroencephalography (EEG) signals, in order to match the blood oxygen level dependent (BOLD) activation to event related potentials. For such applications, the data from the accessory device need to be available in a standardized format and be synchronized with the MR images or the raw k-space data, e.g. time stamps with a common reference should be available for the MR data and the accessory data. For advanced reconstruction methods, such as motion correction, software communication interfaces are necessary between the accessory device and the MR reconstruction software, which can be vendor dependent, or a third-party reconstruction system such as Gadgetron (18).

Several computer and electronics systems have been proposed and have succeeded in achieving many of these requirements, for applications in cardiac MRI (19), patient monitoring (20) or fMRI (21,22). Additionally, systems have been proposed for real-time MRI reconstruction, e.g. Gadgetron, RTHawk (23) (which allows on-the-fly changing of imaging parameters using camera data (24)). However, to the best of our knowledge, none of the listed systems includes the use of accessory devices for MRI reconstruction. To ease the comparison of different devices and methods, and to ease the deployment of systems using accessory devices to other sites, it would be desirable for the MR community to have a standardized, scalable architecture for such systems, standardized communication interfaces and standardized data formats. In particular, a system that could be easily interfaced with many different types of external devices (e.g. ECG, motion tracking devices, microphones, RF or magnetic field gradient probes etc.) and with the Gadgetron open-source reconstruction system is lacking and would be of interest for the image reconstruction community.

The objective of this work is to propose a flexible hardware and software architecture to acquire, record, process (in real-time) and send data from accessory devices and MRI events, which we call signal analyzer and event controller (SAEC). In addition, we propose standardized communication interfaces between accessory devices and SAEC, between SAEC and MR scanner, and between SAEC and Gadgetron. Standardized data formats are also proposed for saving the accessory data (raw and real-time processed data), information about the acquisition devices and settings, and about the real-time processing modules that were used. After describing the hardware and software architecture of the system, we assess its performance in exemplary applications, including cardiac MRI using advanced real-time ECG denoising, real-time speech imaging, and online motion-corrected reconstruction (nonrigid motion) with Gadgetron from free-breathing MRI.

METHODS

System design and implementation

The system described in this paper is partially based on a previous system version described in (7). The older version was based on a PXI system with a LabVIEW (National Instruments, Austin, Texas, USA) software. Given the limitation of the previous system, including scalability, maintenance issues and license cost, the system architecture was completely updated. In this section we describe a solution that, due to the introduction of independent modules, enables easy scalability and high flexibility of the SAEC system.

Hardware description

The hardware platform comprises: (i) a set of sensors/devices, (ii) an electronics module responsible for signal conversion (SAEC Box), (iii) a server that runs the real-time software (SAEC server), and (iv) one or several clients (SAEC clients) that can receive data streams (display of the signals in a user interface), and send commands to the server (configuration of devices, signal processing pipelines, Gadgetron communication etc.) . A schematic representation of the SAEC is depicted in Figure 1a. In order to provide scalability, the communication protocol between the SAEC box and the SAEC server was chosen to be the universal serial bus (USB) protocol. USB provides high compatibility, medium latency (1 ms (25)) and high communication speed but at the cost of a relatively high jitter. Three types of hardware interfaces between the SAEC and the external devices are proposed and implemented in the current version:

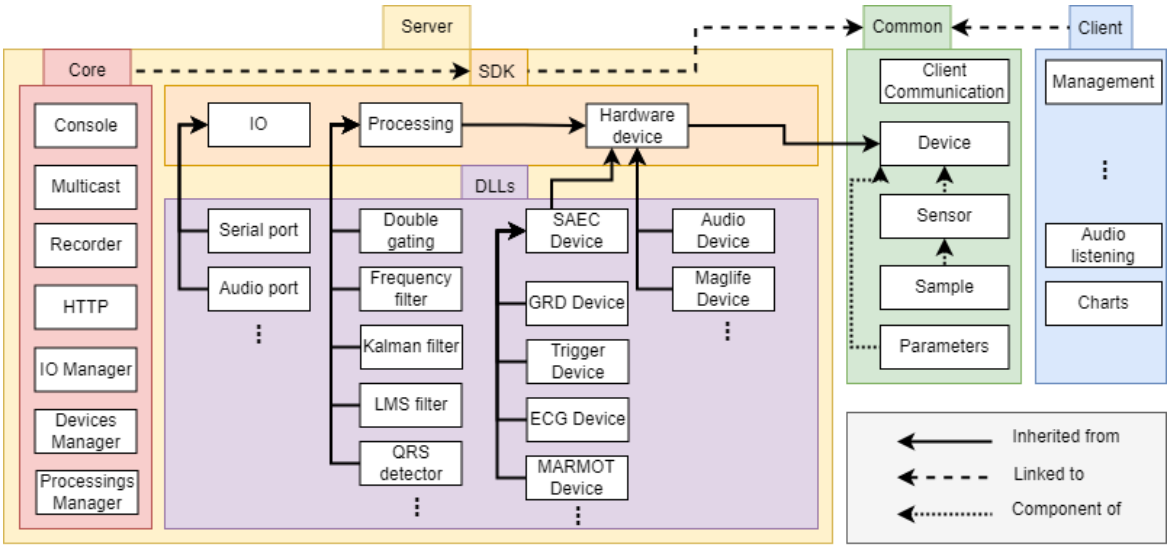

Figure 2. Simplified scheme of software components.

i) The first type of hardware interface is an easy-to-implement solution for devices sending/receiving data through optical fibers. This solution is commonly used with MRI-compatible sensors located within the scan room, as it prevents interferences with the MRI hardware. Examples of such sensors are shown in Figure 1b. Data transmission is achieved with a serial protocol over plastic optical fibers (wavelength 650 nm) with up to 125 Mbd (bd=baud is number of signaling events per second) full duplex communication. The hardware interface consists of a dedicated electronic board, designed to convert between serial and USB with an FTDI chip (Future Technology Devices International Ltd, Glasgow, United Kingdom). The transceivers (Broadcom Inc, San Jose, California) have a higher baud rate than the sensors, so that there is no delay introduced during conversion. We reconfigured the serial protocol for energy saving purpose (reverting signals given that idle state in serial protocol is logic high (1)). Example of such devices currently include ECG sensors (Schiller Médical, Wissembourg, France), and home-made motion sensors using inertial measurement units (accelerometers and gyroscopes) (2).

ii) The second type of hardware interface is a generic solution for devices sending/receiving data through various transportation channels, such as analog or digital IO (inputs/outputs), optical fibers, USB or ethernet. Connection and conversion are performed on dedicated electronic boards for each device, whose main component is an STM32 ARM (Advanced RISC Machine) microcontroller (STMicroelectronics, Grenoble, France). The board directly communicates with the SAEC server through a USB protocol. Devices currently using that interface include (i) a home-made trigger card (Triggers) that can send/receive various trigger signals to/from the MR scanner (in this work, a 3T Prisma scanner from Siemens Healthineers, Erlangen, Germany) via optical fibers. The signals that can be acquired with the "Triggers" card include sequence start, sequence stop, PMU (Patient Monitor Unit) signals which correspond to the vendor's R-wave peak detection, and trigger signals for functional MRI applications. The signals that can be sent include the external trigger inputs of the MRI system, located in the scan room or in the MRI electronics backroom. (ii) A home-made gradient card (GRD HF) was also developed to acquire the currents driving the gradient coils (see Figure 2). The "GRD HF" card used an analog-to-digital converter (ADC) of the STM32 ARM chip. The sampling rate can be configured between 1 and 70 kHz in real time, combined with an analog low-pass 5th order Butterworth filter with adjustable cut-off frequency in the range 0.5-35 kHz for anti-aliasing purpose.

iii) The third type of hardware interface is a direct USB connection to the SAEC server, i.e. it is not part of the SAEC box. Only one device currently uses this interface: an opto-acoustic microphone, which directly connects the manufacturer's output (FOMRI III, Optoacoustics Ltd., Mazor, Israel) by USB to the SAEC server.

Embedded software

Embedded software is needed to manage data transmission using a specific protocol, on the external device side, and on the SAEC side when the generic hardware interface is used (using the STM32 ARM processors). For home-made devices, we also used STM32 ARM chips on the device side. Therefore, the embedded software was based on STMicroelectronic SDK. The embedded system did not use any operating system, since DMA (direct memory access) and interruptions with a priority system provide a better timing precision for the data acquisition and transfer. In order to preserve the devices' battery energy, the sensors do not perform any computations, and their function is restricted to reading data from its peripheral components and sending them directly to the optical serial medium. The proposed communication protocol is described in Support Information S1.

Software description

The software was written in C/C++ and was based on the Qt Framework (v. 5). The general architecture of the software is depicted in Figure 2 and the details are provided in Support Information S1. The SAEC system exploits client-server architecture to ensure correct real-time management. The server core is represented by several classes, including the *Multicast* class (which enables real-time data sending simultaneously to multiple clients) and the *HTTP* interface (which enables data conversion, download and transfer to other systems, such as Gadgetron (18) or ArchiMed research database (26)). Devices are represented in form of dynamically linked libraries and contain implementations of software communication protocols and the protocol for detecting the device type. A *Processing* represents an implementation of a virtual device. A *Processing* can receive, process and send computed data in the same way as if it were a real device, for example double gating (i.e. cardiac-respiratory gating), Frequency filter (low-pass and high-pass filters), LMS (least mean squares) adaptive filter for ECG denoising (27), QRS detector, etc.

The main client that is currently used at our institution provides the user with a generic graphical user interface, including a real-time display of all device data in the form of charts (as illustrated in Figure 3), managing the connection to SAEC server, pausing, data recording, creation of processing tasks and access to all SAEC client settings. Trigger signals can be accompanied by audio or/and

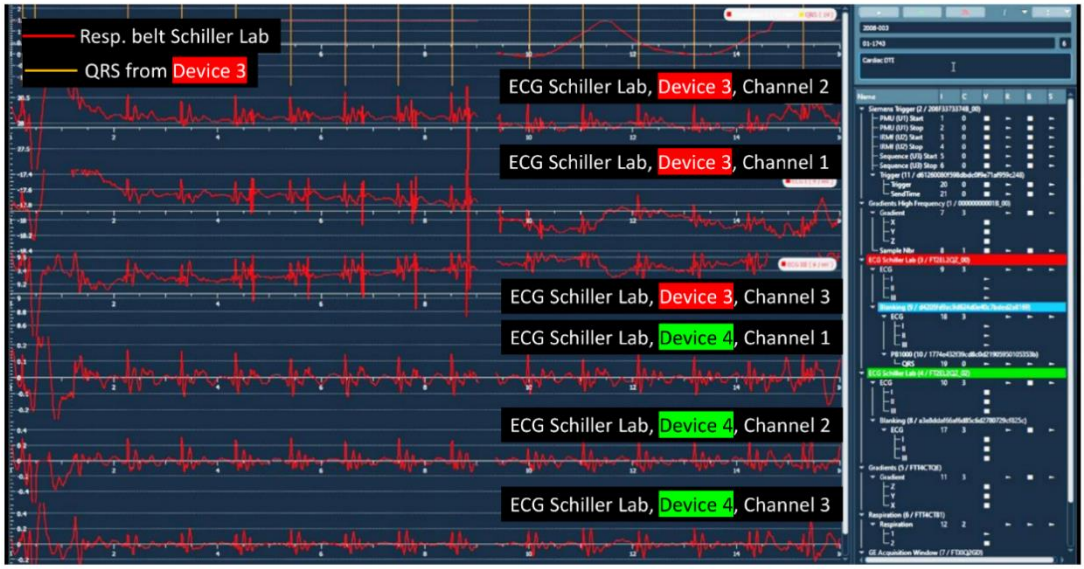

Figure 3. Graphical user interface of the SAEC client in process of an ECG acquisition during a cardiac MRI. The upper row on the chart area shows respiratory data and QRS detection and the lower rows contain denoised ECG.

visual stimuli. The sound from the microphone can be optionally listened to using the speakers of the client computer.

A Client could also be a program that sends instructions to the SAEC server automatically for use by the MR pulse sequence program or by the image reconstruction program such as Gadgetron (see Figure 4 real-time fashion). However, in the proposed implementation, communication between the SAEC and the Gadgetron for online reconstruction was rather handled through an HTTP class (Figure 4 retrospective application). The SAEC server is configured to run in "automatic recording" mode, meaning the SAEC recording starts automatically after reception of a sequence start TTL command. If k-space acquisition successfully starts, a dedicated gadget sends an URL request to the SAEC server, confirming the recording should continue (and that it was not an adjustment sequence). After reception of the last k-space line, the gadget sends a confirmation that the MR acquisition has finished as well as additional meta-information (e.g. protocol name). Once this command has been received, the SAEC server stops the recording and automatically starts raw data conversion to HDF5 format (see next section). Another gadget runs an FTP server and waits for reception of a SAEC file. Upon file reception, the reconstruction using the external device data can be performed. An example source code using this pipeline is published on GitHub https://github.com/IADI-Nancy/Gadgetron.

Data format

We propose to use the hierarchical data format (HDF5) (28) to store all the SAEC data. It is well suited to store metadata together with the data and provides compactness in terms of disk space. Standard readers (e.g. HDFView) and libraries are available in multiple programming languages (C++, Python, MATLAB). The format is schematically illustrated in Figure 5 and the details are provided in Support Information File S1. The source code for the SAEC HDF5 reader, writer, as well as a WFDB (waveform database, a popular format for storing physiological signals) to HDF5 converter, are available on GitHub https://github.com/IADI-Nancy/wrapperHDF5. An example file is also provided in the Support Information File S2.

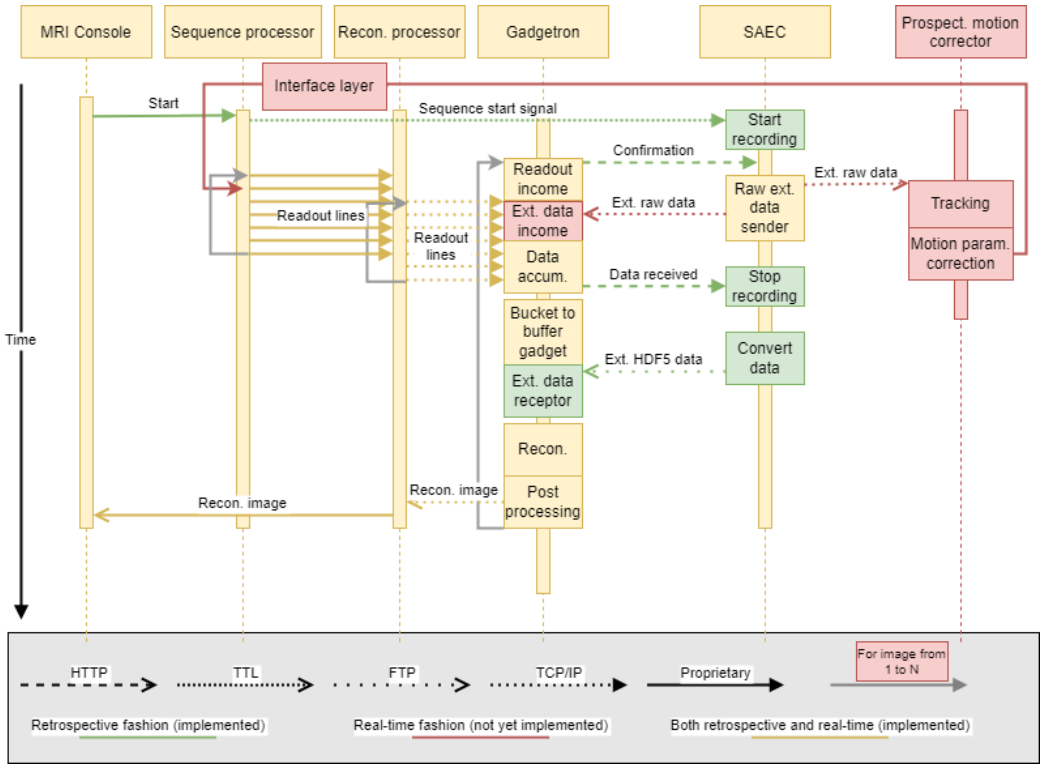

Figure 4. Diagram of the different components communication sequence which enables automatic recording of SAEC files and online reconstruction. The green and the yellow components and connections denote the implemented part. The red components and connections show potential possibilities of the proposed system which are not yet implemented in out laboratory.

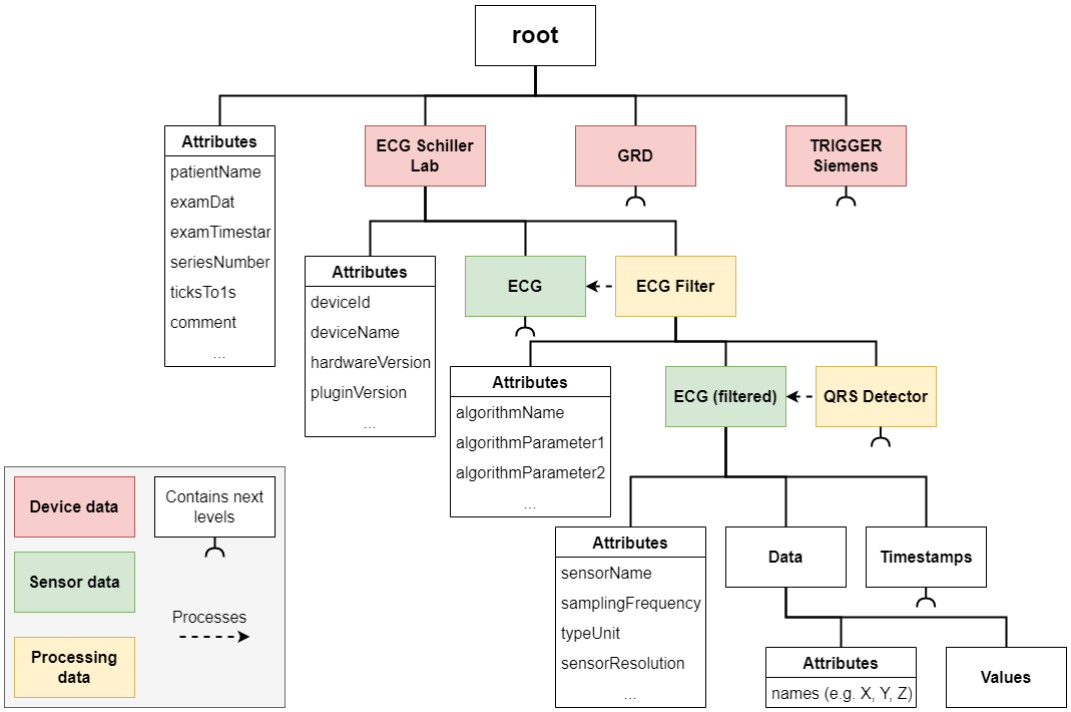

Figure 5. Data format schematically illustrated on the example file with ECG filtering and QRS detection (provided in Supporting Information File S2).

System validation

In order to validate the SAEC system, we performed several experiments designed to evaluate its performance and show its versatility and demonstrate potential applications. The main objectives were: (i) to ensure the accuracy of the acquired data (ii) to assess the latency of the real-time system (delay, jitter); (iii) to ensure synchronicity between MRI data and external device data (iv) to demonstrate the feasibility of advanced real-time processing of external data; (v) to demonstrate online reconstruction capabilities with Gadgetron using the SAEC data.

Integration to the MR system

The SAEC system was set up on a Siemens 3T platform (Prisma, Siemens Healthineers, Erlangen, Germany). The SAEC server was installed on a computer (24 cores, 2.3 GHz, 64 Gb of RAM) equipped with Linux operating system (Debian v.10) located in the MR electronics backroom. The SAEC client providing graphical user interface was installed on a computer (6 cores, 3.3 GHz, 8 Gb of RAM, no dedicated GPU) equipped with Windows 10 (Microsoft, Redmond, USA), located next to the MR console. The SAEC server was connected to the MRI system through several hardware interfaces, as mentioned in the previous section: (i) external trigger input located in the scan room; (ii) MR inputs/outputs (MR gradients, PMU signals, external trigger) located in the electronics backroom; (iii) ethernet communication through the internal network of the MR system, which was shared by the MR console, the MR vendor's measurement and reconstruction system (MARS), the SAEC server, and a Gadgetron (v. 4) reconstruction server. For the experiments described in the remainder of the text, the following accessory devices were connected to the SAEC (when needed, according to the application): an ECG sensor prototype from the Maglife system (Maglife Serenity, Schiller Médical, Wissembourg, France), a pneumatic respiratory belt connected to the Maglife system (optical fiber transmission to the SAEC box), an opto-acoustic microphone (FOMRI III, Optoacoustics Ltd., Mazor, Israel).

All data involving human subjects were collected within the "METHODO" study (ClinicalTrials.gov Identifier: NCT02887053) approved by the institutional ethics review board (CPP EST-III, 08.10.01). All participants provided written informed consent.

Comparison between simulated and recorded MR gradient pulses

To validate the accuracy of the recordings, we first compared our SAEC-based high-frequency acquisition (70 kHz) of the MR gradients to the simulated gradient waveforms obtained from the vendor's pulse sequence development software (Siemens' IDEA, software version VE11C). A dedicated sequence was developed with well-distinguishable trapezoidal gradient waveforms. The simulated and measured signals were manually aligned in time (global translation) and rescaled (with a global scaling factor) to check the fidelity of the measured waveforms.

Delays of the SAEC system

Delays introduced by the SAEC system during real-time operation need to be quantified. The total delay Δt_{total} can be expressed as:

$$\Delta t_{total} = \Delta t_{read} + \Delta t_{proc} + \Delta t_{write},$$

where Δt_{read} is the delay introduced by reading the device data, Δt_{proc} is the delay introduced by the real-time processing, and Δt_{write}, when applicable, is the delay introduced by writing the data to an output channel (e.g. trigger send to the MR system). Δt_{proc} depends on the application and the processing algorithms. Δt_{read} and Δt_{write} are variable delays inherent to the use of the USB protocol. This variable delay is expected to be on the order of 1 ms. It should also be noted that, as a consequence, when high-frequency sampling is required (typically > 1 kHz), data will be sent and read in packets of multiple samples. The SAEC server labels all data samples from a given packet with the same time stamp. Therefore, a resampling of the data is necessary when reading a SAEC file recording, to account for both the USB delay and the transmission of data in packets.

These delays were estimated by analyzing the timestamps provided by the SAEC server upon USB reading and USB writing. Since the device data are emitted with hardware-controlled timings and transferred through optical fibers, the data should be received by the SAEC box with a constant delay (i.e. with no jitter), so it is assumed that the variations in delays are induced by the USB communication. Therefore, we expressed Δt_{read} as delay between consecutive timestamps associated with the device data reading

(expressed as mean +/- standard deviation). We may assume that $\Delta t_{write} = \Delta t_{read}$. Finally, the original timestamp of the device data is stored through the processing pipeline. Therefore, upon USB writing (e.g. TTL trigger sent to the scanner), the current timestamp can be compared to the original timestamp (obtained at USB reading) of the data sample. The difference directly provides Δt_{proc}.

Multimodal vocal tract acquisition (MRI, sound, and physiology)

A first application of the SAEC is given in the context of real-time imaging of the vocal tract. A volunteer was asked to sing during a real-time MRI sequence. Sound and respiration were recorded with the SAEC and retrospectively post-processed. The real-time sequence was a spoiled gradient echo sequence (2D FLASH) with a highly undersampled radial sampling scheme, with the following parameters: TE/TR = 1.47/2.22 ms, 5° flip angle, 136x136 matrix size, 9 radial spokes per frame, 1.6 mm in-plane resolution, 8 mm slice thickness, 20 ms/frame temporal resolution. A real-time non-linear reconstruction (29) was performed with a dedicated reconstruction server. The sequence start and stop signals allowed all the SAEC external data to be easily synchronized with MR images for retrospective analysis. Qualitative evaluation of the multimodal data was performed.

Real-time ECG denoising for prospectively gated cardiac MRI

Prospective real-time use of the SAEC was evaluated by prospectively gating cardiac MRI using an external ECG device, and advanced signal processing. The ECG device was a prototype from the Maglife system (Schiller Médical, Wissembourg, France), which was designed to acquire data at 16 kHz (30). This broadband acquisition technique has been shown to improve the removal of strong ∂B/∂t spike artifacts which are not removed by conventional filtering at lower bandwidth. The SAEC acquired the raw ECG data at 16 kHz, and performed real-time denoising (using a method similar to that in (30)) followed by filtering and downsampling to 1 kHz. The denoised ECG signal was entered into a simple QRS detection algorithm (bandpass between 15 and 40 Hz and peak detection with a manually selected minimum peak height). Finally, the resulting TTL signal was sent to the external trigger input of the MR system using the SAEC "Triggers" card. Then, the sequence was repeated with the vendor's built-in ECG gating. The MR gradients were also recorded to capture the feedback from the MR sequence. The sequence was repeated 5 and 8 times, respectively, during 2 experiments with the same volunteer, and the standard ECG sensor was installed by professional MRI technologists. The MR sequence was a prospectively gated cardiac phase sensitive inversion recovery (PSIR) sequence, with the following parameters: 256x200 matrix size, TE = 1.17 and TR = 858/700 ms (different for two experiments), 1.6 mm in-plane resolution, 8 mm slice thickness, 1 slice (short-axis), trigger time = 745/585 ms, acquired within a breath hold.

Online MRI reconstruction using physiological data from accessory devices

Online MRI reconstruction with Gadgetron was tested in a breast MRI application. The volunteer was lying in supine position, an 18-channel cardiac coil was used in combination with the spine coil elements integrated to the exam table, and respiratory motion correction was required. A T2-weighted 2D turbo spin echo (TSE) sequence was used with the following parameters: 320x448 matrix size, TE/TR = 97/5970 ms, 0.72 mm in-plane resolution, 2 mm slice thickness (0.4 mm gap), 80 slices (whole breast coverage), turbo factor = 18. The acquisition lasted 6 min 20 sec and was performed during free breathing. Nonrigid motion-corrected reconstruction was achieved with the GRICS technique (31). GRICS allows the joint reconstruction of the motion-free image and a motion model, based on the signal from the MARMOT accelerometer (2) which is shown in Figure 8. The reconstruction was performed on a machine with 96 cores (3.7 GHz CPUs) and 256 GB RAM, located outside of the MRI network and accessible from Gadgetron through SSH tunneling.

The delays for the online reconstruction were obtained by comparing the Gadgetron and Siemens log-files. The baud rate of both networks was 1 Gbd and the total latency (sum of delays evaluated with "ping" command) was around 0.5 ms. Transfer delays were calculated from 10 repetitions.

RESULTS

SAEC recording of MR gradients

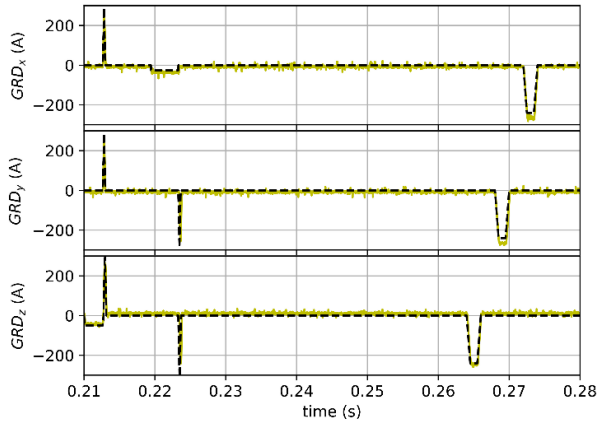

Figure 6. Recorded *x*, *y* and *z* components of gradient currents. The dashed black line represents the simulated waveforms using the vendor's development environment, the solid yellow line corresponds to the measured currents.

Figure 6 shows the measured gradient waveforms with SAEC, alongside the simulated waveforms provided by the pulse sequence environment. The measured and simulated signals are in good agreement. Visually, the communication protocol does not seem to have any impact on the temporal fidelity of the acquired signals.

SAEC delays

The USB jitter (corresponding to the standard deviation of Δt_{read}) was measured to be 0.067 ms for the gradient acquisition board (with a 70 kHz sampling frequency), and 0.242 ms for the ECG device (with 16 kHz sampling frequency). Further details on mean difference between timestamps, and other statistics for different sampling frequencies are assembled in Table 1. The total processing delay, in case of real-time ECG denoising with QRS detection and trigger generation, was 0.208±0.203 ms.

Sampling frequency	Mean, ms	SD, ms	Max, ms
1 kHz	0.984	0.140	2.088
16 kHz	0.063	0.242	1.171
70 kHz	0.015	0.067	2.209

Table 1. Information about mean read time, standard deviation (jitter) and maximal read time using the SAEC system for different sampling frequencies.

Multimodal acquisition of the vocal tract

An example video of real-time MRI of the vocal tract during singing, with corresponding denoised sound and respiration curves, is provided in the Supporting Information Video S1.

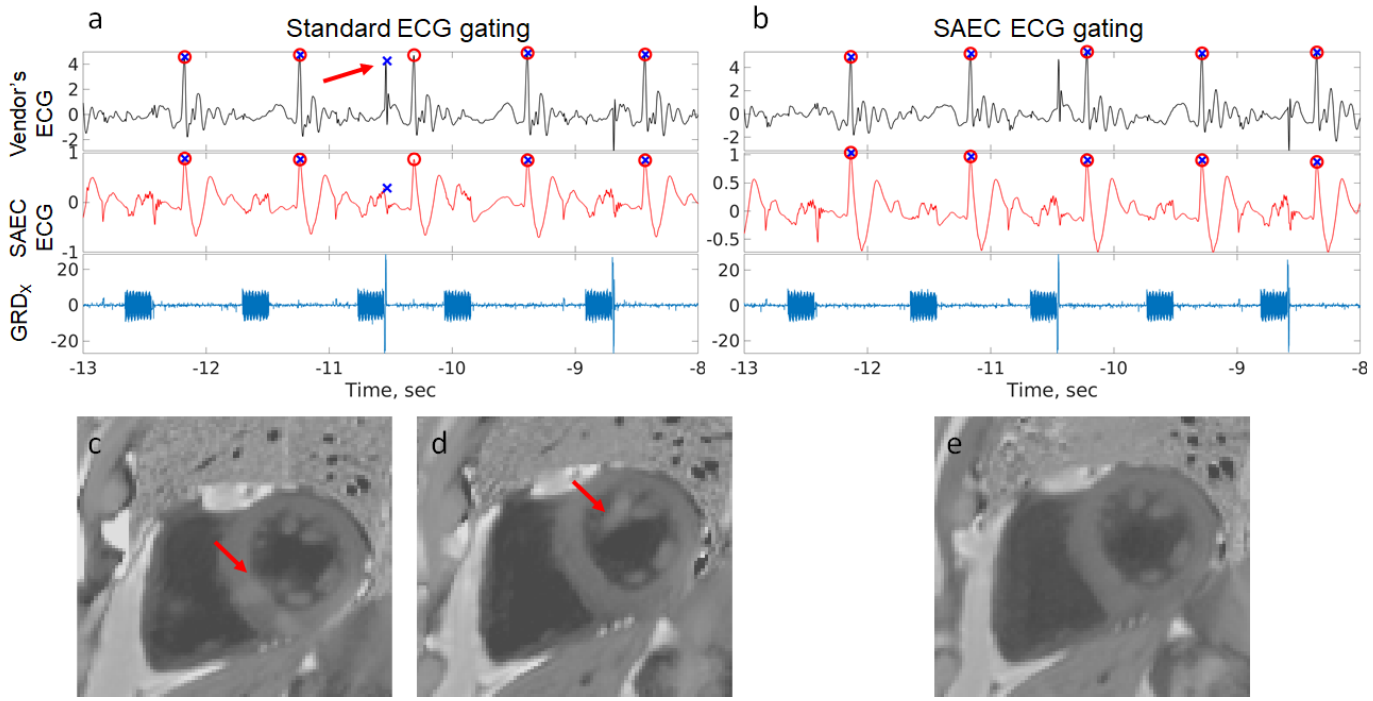

Figure 7. (a) Example of erroneous standard QRS detection acquired during a ECG-gated sequence. The upper plot shows vendor's ECG distorted by residual gradient spike artifacts (black line), the middle plot depicts denoised ECG acquired with the SAEC system (red line), and the lower plot shows the x-component of the gradient field recorded with the SAEC system (blue line). Black crosses correspond to standard vendor's QRS detection and red circles denote SAEC QRS detection. Only a part of the sequence is shown on the plot. (b) Example of ECGs acquired during a sequence gated with the SAEC system. (c) ROI of an image acquired in course of the first experiment, gated with the standard ECG, with one false positive and one false negative QRS detection. (d) ROI of an PSIR image acquired in course of the second experiment, gated with the standard ECG, with one false positive QRS detection. The ECGs from the plot (a) correspond to this MR image. (e) ROI of an PSIR image acquired in course of the second experiment, gated with the SAEC. The ECGs from the plot (b) correspond to this MR image. All artifacts are shown with the red arrows.

Real-time ECG denoising and cine MRI

For each experiment, one of the images acquired with the standard gating (that is 15% of the acquired images) was distorted by artifacts due to incorrect R-peak detection (approximately 120 ms earlier for the first experiment and 250 ms earlier for the second experiment). This mis-detection can be explained by presence of residual gradient-induced artifacts on the conventional ECG (see Figure 7). These artifacts were, however, successfully removed from the signal acquired with the accessory ECG sensor and the resulting images were thus artifact-free.

Online reconstruction with Gadgetron

An example online reconstruction of breast MRI data, using Gadgetron and SAEC, is depicted in Figure 8, alongside the vendor's reconstruction. This example highlights the efficient reduction of the motion-induced blurring artifacts by the online reconstruction, in a large field-of-view covering both breasts. The online reconstruction took 2 min, which was short compared to the acquisition time (6 min 20 s). Data transfer through the network took less than 2 seconds (1.14 seconds in average) which was negligible in comparison to the reconstruction time.

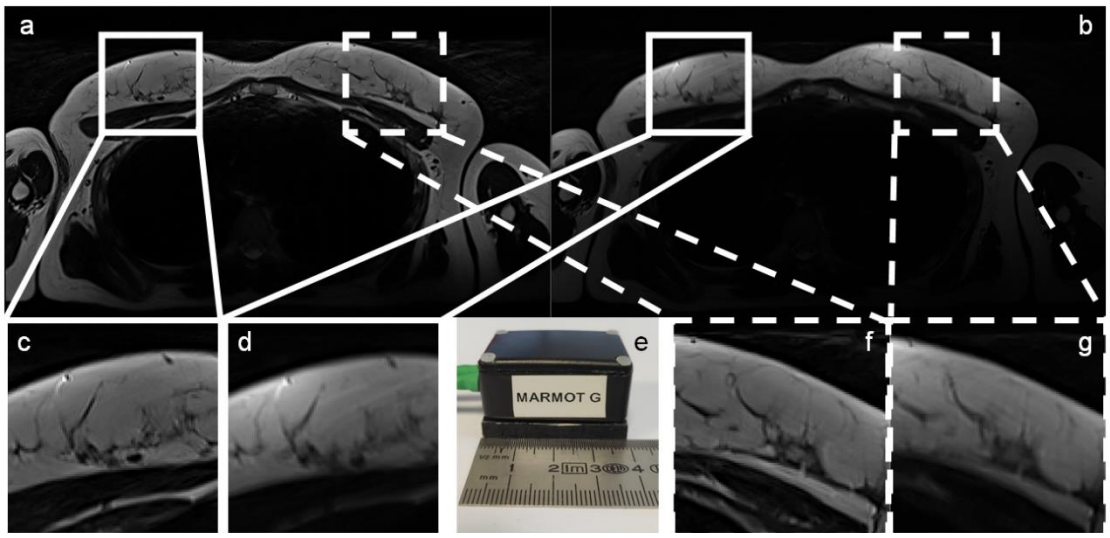

Figure 8. a) Example of motion-corrected image reconstructed online with usage of external accelerometer data. b) Standard Siemens reconstruction. c), f) Zoomed regions of the motion-corrected image denoted by solid and dashed rectangles. d), g) The same regions, taken from the image without motion correction. e) MARMOT accelerometer sensor used for respiratory data acquisition.

DISCUSSION

The proposed system and architecture have been shown to reliably acquire both external and MRI data synchronously with the MRI imaging data. Contrary to numerous existing systems which focus on one application (e.g. adjustment of sampling trajectory using patient's cardiac rhythm (32) or gating based on knee contraction force (33)), the SAEC system is a generic scalable solution which supports easy inclusion of any device supporting real-time communication protocol (serial, ethernet). The different example applications have shown the overall versatility of the system, and possible applications are not limited to those already implemented and highlighted in this paper. One could for example envision the use of dedicated sensor (34) or direct connection to the MR scanner for the acquisition of RF signals, for monitoring the ongoing pulse sequence. Another possible use of the SAEC would be to prospectively control and correct the MRI acquisition to compensate for out-of-plane motion with real-time acquisition and processing of external physiological data.

We provided a proof-of-concept example when utilization of an accessory ECG sensor and a homemade denoising algorithm allowed us to avoid spike artifacts on ECG which improved imaging quality. Even if these artifacts were not always classified as R-peaks by the standard QRS detector, ensuring that the image was artifact-free required an additional retrospective ECG check which is not systematically done in clinical practice. Utilization of an external system with control over algorithms and parameters provides flexibility, oppositely to clinical built-in devices and algorithms. This can be crucial in case of non-standard usage of ECG gating, e.g. for brain MRI (with greater distance of the sensor from the field isocenter).

We demonstrated that it is possible to perform an online MRI reconstruction with a direct communication with the Gadgetron system. Our exemplary application was free-breathing supine breast MRI. Contrary to conventional prone position, supine position is adopted for ultrasonic examination, biopsy or mastectomy, and supine position is also more comfortable for the patient. However, the presence of motion artifacts could render the image almost uninterpretable. We have shown that the proposed setup allows fast and efficient motion correction therefore ensuring good image quality. The compactness of the motion sensor exploited for this experiment makes it possible to install it on any point of the body or on a flexible coil that makes it advantageous over a respiratory belt provided by MRI vendors. We were interested in retrospective motion correction and did therefore not implement real-time physiological data transfer; however, considering existing implementation of data broadcast on the SAEC server, this option would only require implementing a client and additional Gadgetron writers and readers for data transfer between gadgets. In our case, reconstruction gadget was based on the GRICS algorithm; however, it could be replaced by other reconstruction techniques relying on external data, for example, k-space sort or discard based on ECG or respiratory data, or trajectory correction for non-cartesian sampling schemes using gradient waveforms information.

The proposed HDF5 format for external data storage had multiple advantages over other existing formats in context of the application discussed in the present paper. For example ISMRMRD (35) can also be used to store waveform data acquired with an MRI system. However, it is not well-suited for external devices as timestamps and measurement identifiers are based on those of the MRI system; clock synchronization between the different systems would therefore be problematic. Numerous metadata fields, such as device description, would also be missing. Data formats suggested for physiological signals, such as WaveForm DataBase (WFDB) (36), EDF+ (37), HL7 aECG (38) are adapted mostly for utilization with well calibrated clinical devices, and also based on a common clock (even though multi-frequency signals are possible). The lack of timestamps associated with the physiological data can be critical in case of imperfect devices (or in-house prototypes), which could be having delay issues or intermittent losses of data portions, which can lead to large distortions of the recorded data and render the recording unusable.

Contrary to real-time streaming tools designed for interventional MRI, such as OpenIGTLink (39), which works with high-level message datatypes, the SAEC system transmits messages of minimal size and overhead which reduces transfer delays. The USB communication jitter, which was low across all the sampling frequencies currently used by the in-house external devices, and the reasonable processing time ensures acceptable delays and variability of emitted control signals, even for time-critical applications such as prospective cardiac gating. Further improvements can include replacing USB connectors with an Ethernet communication protocol, which would further reduce the data transfer jitter and increase baud rate (for the transmission of high frequency signals such as RF pulses).

CONCLUSION

We proposed a complete system for acquiring external device data during MR imaging, with a wide range of functionalites. The proposed hardware configuration ensures the system scalability and also ensures reliable measurements and transmission of external device and MRI data (MRI trigger events, gradient command signals, ECG,...). The proposed hardware and software solutions make it possible to record, process (in real-time) and send signals from external devices, simultaneously and synchronously with MRI acquisitions. Standard and flexible data formats and communication protocols were proposed. Delays and jitters of the system were low (on the order of a millisecond) which is acceptable for most clinical applications. Finally communication with Gadgetron was shown to allow efficient online image reconstruction, using techniques relying on physiological data from external devices.

REFERENCES

1. Maclaren J, Herbst M, Speck O, Zaitsev M. Prospective motion correction in brain imaging: a review. Magn. Reson. Med. 2013;69:621–636.
2. Chen B, Weber N, Odille F, et al. Design and validation of a novel mr-compatible sensor for respiratory motion modeling and correction. IEEE Trans. Biomed. Eng. 2016;64:123–133.
3. Preiswerk F, Toews M, Hoge WS, et al. Hybrid utrasound and MRI acquisitions for high-speed imaging of respiratory organ motion. In: International Conference on Medical Image Computing and Computer-Assisted Intervention. Springer; 2015. pp. 315–322.
4. Zhu Y, Kim Y-C, Proctor MI, Narayanan SS, Nayak KS. Dynamic 3-D visualization of vocal tract shaping during speech. IEEE Trans. Med. Imaging 2012;32:838–848.
5. Niebergall A, Zhang S, Kunay E, et al. Real-time MRI of speaking at a resolution of 33 ms: undersampled radial FLASH with nonlinear inverse reconstruction. Magn. Reson. Med. 2013;69:477–485.
6. Isaieva K, Laprie Y, Leclère J, Douros IK, Felblinger J, Vuissoz P-A. Multimodal dataset of real-time 2D and static 3D MRI of healthy French speakers. Sci. Data 2021;8:258 doi: 10.1038/s41597-021-01041-3.
7. Odille F, Pasquier C, Abacherli R, Vuissoz P-A, Zientara GP, Felblinger J. Noise Cancellation Signal Processing Method and Computer System for Improved Real-Time Electrocardiogram Artifact Correction During MRI Data Acquisition. IEEE Trans. Biomed. Eng. 2007;54:630–640 doi: 10.1109/TBME.2006.889174.
8. Oster J, Pietquin O, Kraemer M, Felblinger J. Nonlinear Bayesian filtering for denoising of electrocardiograms acquired in a magnetic resonance environment. IEEE Trans. Biomed. Eng. 2010;57:1628–1638.
9. AlMahamdy M, Riley HB. Performance study of different denoising methods for ECG signals. Procedia Comput. Sci. 2014;37:325–332.

10. Schmidt M, Krug JW, Rose G. Reducing of gradient induced artifacts on the ECG signal during MRI examinations using Wilcoxon filter. Curr. Dir. Biomed. Eng. 2016;2:175–178.
11. Chia JM, Fischer SE, Wickline SA, Lorenz CH. Performance of QRS detection for cardiac magnetic resonance imaging with a novel vectorcardiographic triggering method. J. Magn. Reson. Imaging 2000;12:678–688.
12. Oster J, Pietquin O, Abacherli R, Kraemer M, Felblinger J. A specific QRS detector for Electrocardiography during MRI: using Wavelets and Local Regularity Characterization. In: 2009 IEEE International Conference on Acoustics, Speech and Signal Processing. IEEE; 2009. pp. 341–344.
13. Schmidt M, Krug JW, Gierstorfer A, Rose G. A real-time QRS detector based on higher-order statistics for ECG gated cardiac MRI. In: Computing in Cardiology 2014. IEEE; 2014. pp. 733–736.
14. Dold C, Zaitsev M, Speck O, Firle EA, Hennig J, Sakas G. Advantages and limitations of prospective head motion compensation for MRI using an optical motion tracking device. Acad. Radiol. 2006;13:1093–1103.
15. Aksoy M, Forman C, Straka M, Çukur T, Hornegger J, Bammer R. Hybrid prospective and retrospective head motion correction to mitigate cross-calibration errors. Magn. Reson. Med. 2012;67:1237–1251.
16. Odille F, Uribe S, Batchelor PG, Prieto C, Schaeffter T, Atkinson D. Model-based reconstruction for cardiac cine MRI without ECG or breath holding. Magn. Reson. Med. 2010;63:1247–1257.
17. Richter JA, Wech T, Weng AM, et al. Free-breathing self-gated 4D lung MRI using wave-CAIPI. Magn. Reson. Med. 2020;84:3223–3233.
18. Hansen MS, Sørensen TS. Gadgetron: an open source framework for medical image reconstruction. Magn. Reson. Med. 2013;69:1768–1776.
19. Kakareka JW, Faranesh AZ, Pursley RH, et al. Physiological recording in the MRI environment (PRiME): MRI-compatible hemodynamic recording system. IEEE J. Transl. Eng. Health Med. 2018;6:1–12.
20. Lee H-C, Jung C-W. Vital Recorder—a free research tool for automatic recording of high-resolution time-synchronised physiological data from multiple anaesthesia devices. Sci. Rep. 2018;8:1–8.
21. Mirsattari SM, Ives JR, Bihari F, Leung LS, Menon RS, Bartha R. Real-time display of artifact-free electroencephalography during functional magnetic resonance imaging and magnetic resonance spectroscopy in an animal model of epilepsy. Magn. Reson. Med. Off. J. Int. Soc. Magn. Reson. Med. 2005;53:456–464.
22. Purdon PL, Millan H, Fuller PL, Bonmassar G. An open-source hardware and software system for acquisition and real-time processing of electrophysiology during high field MRI. J. Neurosci. Methods 2008;175:165–186.
23. Santos JM, Wright GA, Pauly JM. Flexible real-time magnetic resonance imaging framework. In: The 26th Annual International Conference of the IEEE Engineering in Medicine and Biology Society. Vol. 1. IEEE; 2004. pp. 1048–1051.
24. Qin L, Gelderen P van, Derbyshire JA, et al. Prospective head-movement correction for high-resolution MRI using an in-bore optical tracking system. Magnetic Resonance in Medicine. https://onlinelibrary.wiley.com/doi/abs/10.1002/mrm.22076. Published October 1, 2009. Accessed July 1, 2019 doi: 10.1002/mrm.22076.
25. Anderson D, Dzatko D. Universal Serial Bus System Architecture. MindShare INC; 2001.
26. Micard E, Husson D, Team C-I, Felblinger J. ArchiMed: a data management system for clinical research in imaging. Front. ICT 2016;3:31.
27. Abächerli R, Pasquier C, Odille F, Kraemer M, Schmid J-J, Felblinger J. Suppression of MR gradient artefacts on electrophysiological signals based on an adaptive real-time filter with LMS coefficient updates. Magn. Reson. Mater. Phys. Biol. Med. 2005;18:41–50.
28. The HDF Group. Hierarchical data format version 5. http://www.hdfgroup.org/HDF5. Published 2000.
29. Uecker M, Zhang S, Voit D, Karaus A, Merboldt K-D, Frahm J. Real-time MRI at a resolution of 20 ms. NMR Biomed. 2010;23:986–994 doi: 10.1002/nbm.1585.
30. Dos Reis JE, Odille F, Petitmangin G, et al. Broadband electrocardiogram acquisition for improved suppression of MRI gradient artifacts. Physiol. Meas. 2020;41:045004.
31. Odille F, Vuissoz P-A, Marie P-Y, Felblinger J. Generalized Reconstruction by Inversion of Coupled Systems (GRICS) applied to free-breathing MRI. Magn. Reson. Med. 2008;60:146–157 doi: 10.1002/mrm.21623.
32. Contijoch F, Han Y, Iyer SK, et al. Closed-loop control of k-space sampling via physiologic feedback for cine MRI. PLOS ONE 2020;15:e0244286 doi: 10.1371/journal.pone.0244286.
33. Oda T, Malis V, Finni T, Kinugasa R, Sinha S. Dynamics of Quadriceps Muscles during Isometric Contractions: Velocity-Encoded Phase Contrast MRI Study. Diagnostics 2021;11:2280 doi: 10.3390/diagnostics11122280.
34. Barbier T, Piumatti R, Hecker B, Odille F, Felblinger J, Pasquier C. An RF-induced voltage sensor for investigating pacemaker safety in MRI. Magn. Reson. Mater. Phys. Biol. Med. 2014;27:539–549 doi: 10.1007/s10334-014-0437-4.
35. Inati SJ, Naegele JD, Zwart NR, et al. ISMRM Raw data format: A proposed standard for MRI raw datasets. Magn. Reson. Med. 2017;77:411–421.
36. Silva I, Moody GB. An open-source toolbox for analysing and processing physionet databases in matlab and octave. J. Open Res. Softw. 2014;2.
37. Kemp B, Olivan J. European data format 'plus'(EDF+), an EDF alike standard format for the exchange of physiological data. Clin. Neurophysiol. 2003;114:1755–1761.
38. Brown BD, Badilini F, others. HL7 aECG implementation guide. Regul. Clin. Res. Inf. Manag. Tech. Comm. 2005.
39. Tokuda J, Fischer GS, Papademetris X, et al. OpenIGTLink: an open network protocol for image-guided therapy environment. Int. J. Med. Robot. 2009;5:423–434 doi: 10.1002/rcs.274.

SUPPORTING INFORMATION

Supporting Information Video S1. Video with real-time vocal tract MRI acquired simultaneously with sound and respiration. The upper plot shows the respiratory belt indications and the lower plot show the denoised sound. The denoised sound is also present on the audio track of the video.

Supporting Information File S1. Implementation details: Server-device communication protocol, Details on the Software, Data format

Supporting Information File S2. Example of HDF5 SAEC file.

Supporting Information File S3. Doxygen documentation of the SAEC software.